

RadioAstron orbit determination and evaluation of its results using correlation of Space-VLBI observations

M. V. Zakhvatkin^{a,*}, A. S. Andrianov^b, V. I. Kostenko^b, Y. Y. Kovalev^b, S. F. Likhachev^b, A. G. Rudnitsky^b, V. A. Stepanyants^a,
A. G. Tuchin^a, P. A. Voytsik^b, G. S. Zaslavskiy^a

^a*Keldysh Institute of Applied Mathematics RAS, Miusskaya sq. 4, Moscow, Russia 125047*

^b*Astro Space Center of Lebedev Physical Institute of RAS, 84/32 Profsoyuznaya st., Moscow, Russia 117997*

Abstract

Orbit determination (OD) is crucial for very-long baseline interferometry (VLBI) experiments conducted with RadioAstron space observatory. The signals recorded by the spacecraft and an Earth-based observatory are to be correlated, which requires accurate delay modeling and thus adequate knowledge of the spacecraft trajectory. In this paper we describe an OD method which was used with the RadioAstron mission in order to achieve orbital accuracy sufficient for successful operation of the ground-space interferometer. In addition to standard ground-based tracking the method utilizes additional information on thrusters firings, rotation of reaction wheels and current attitude of the spacecraft obtained via telemetry channel. The performance of spacecraft navigation for space VLBI experiments with RadioAstron is evaluated in the context of correlation between signals obtained on the Earth and on the orbit, namely residual values found during correlation processing of more than 5000 data scans recorded over 7 years of the mission. Such data contains information about the orbital errors projected on the direction to the observed radio source.

Keywords: RadioAstron, orbit determination, space-VLBI

1. Introduction

RadioAstron spacecraft featured with 10 metre space radio telescope (SRT) was launched into highly elliptical Earth orbit in July 2011 by means of “Zenit-3F” rocket and “Fregat-SB” upper stage. The main scientific purpose of the spacecraft is to conduct observations of galactic and extragalactic radio sources in conjunction with ground based radio telescopes forming a multi-antenna ground-space radio interferometer with extremely long baselines [Kardashev et al. \(2013\)](#). The spacecraft also provides a great opportunity to test the Einstein Equivalence Principal with its eccentric orbit and installed H-maser as precise atomic clocks on the board [Litvinov et al. \(2018\)](#).

Processing of observational data of the ground-space interferometer involves a fringe search procedure, i.e. search of maximum amplitude of the cross correlation function between signals recorded at different telescopes. Finding the correlation is associated with determination of wavefront arrival delay and its derivatives for involved telescopes throughout the experiment. The initial guess for the delay is calculated according to a model, which utilizes trajectories of phase centers of participating telescopes in the inertial frame, offsets and drifts of their clocks, propagation media parameters and etc. To do the fringe search in reasonable time errors of a priori knowledge of these parameters should be quite limited.

In the particular case considered in this paper one of the telescopes is orbiting the Earth. Therefore the major uncertainty of modelled delay is associated with the orbit determination errors of the spacecraft carrying the SRT. The following level of orbital errors is considered acceptable in terms of fringe search performance: total position error is less than 600 m, total velocity error is less than 2 cm/sec and total acceleration error is less than 10^{-8} m/s².

2. Orbit and dynamics

RadioAstron spacecraft was launched on highly elliptic orbit with apogee distance varying between 280 000 and 340 000 km and perigee height above 650 km. The orbit undergoes significant evolution over time in both eccentricity and orientation of the orbital plane because of luni-solar gravitational perturbations and Earth’s gravitational field during occasional low perigees (see [Table 1](#)). Initially the specific orbit has been chosen to provide opportunities for observation of the variety of most important galactic and extragalactic radio sources with different baseline projections and phase angles. Orbital evolution happens without intentional maneuvers. Only three trajectory correction maneuvers has been performed so far. Their goal was to prolong orbital lifetime preventing reentry during next local minima of perigee height and to prevent unacceptably long shadowing of the spacecraft.

Except for rare moments when the spacecraft is moving near a perigee and perigee height is close to its local minimum the major part of perturbing accelerations are due to gravitational pull of third bodies and non-gravitational accelerations. The

*Corresponding author at: Keldysh Institute for Applied Mathematics, Russian Academy of Sciences, Miusskaya sq. 4, 125047 Moscow, Russia.

Email address: zakhvatkin@kiam1.rssi.ru (M. V. Zakhvatkin)

Epoch	2011-08-21	2012-10-13	2014-01-27	2015-03-23	2016-06-24	2017-07-31	2018-02-17
h_π , km	6.213	69.265	1.075	67.666	0.654	75.716	3.699
h_α , km	336.526	278.126	338.611	280.593	336.278	306.435	329.026
i , deg	56.354	76.804	9.199	56.692	43.866	68.527	51.309
Ω , deg	331.682	295.970	152.397	107.007	0.930	306.140	297.661

Table 1: Evolution of the RadioAstron orbital elements.

latter is less predictable and appears the main source of errors when modelling the dynamics of the RadioAstron spacecraft. Among non-gravitational perturbations solar radiation pressure has the greatest impact on the orbit. Because of 10 metre antenna of the SRT area to mass ratio of the spacecraft can reach 0.03 kg/m^2 with acceleration due to SRP up to $2 \cdot 10^{-7} \text{ m/s}^2$ for certain attitudes with respect to the Sun. The account for the SRP in the dynamics of the RadioAstron is complicated by the fact that its attitude is determined by the observed radio source and may change significantly within several hours.

In addition to direct acceleration SRP produces the major part of perturbing torque. Attitude control of the RadioAstron, which includes compensation of external torques, is implemented with reaction wheels. RadioAstron attitude in the inertial space roughly can be described as piece-wise constant — most of the time the spacecraft is not rotating and external torques are compensated by reaction wheels, and all the attitude changes happen in relatively short time. The motion around the center of mass has been touched because its perturbations are coupled with ones on the motion of the center of mass. Several times a day angular momentum accumulated by reaction wheels reaches the critical values where it is no longer possible to parry external torque further accumulating angular momentum or to perform upcoming attitude change. Every such an event is followed by a desaturation of the angular momentum of reaction wheels, during which reaction wheels nearly stop and resulting rotation of the spacecraft is prevented by means of thrusters. Every desaturation produces net Delta V of 3–7 mm/s and the total effect of velocity change over time is comparable to the one of direct SRP and therefore must be taken into account.

To take proper account for the SRP in the dynamics of the center of mass of the spacecraft we developed an adjustable model which allows to calculate both perturbing acceleration and torque for a given attitude with respect to the Sun [Zakhvatkin et al. \(2014\)](#). The SRP model utilizes simplified model of the surface consisting of SRT parabolic antenna, solar panels and spacecraft bus. With surfaces of the antenna and the bus are associated coefficients of reflectivity α_1 and specularity μ_1 , with the surface of solar panels — coefficient of reflectivity α_2 . The force and torque due to SRP in the spacecraft fixed frame according to the model are as follows

$$\mathbf{F}_{SRP} = \alpha_1(1 - \mu_1)\mathbf{F}_{A,B}^d(\mathbf{s}) + \alpha_1\mu_1\mathbf{F}_{A,B}^s(\mathbf{s}) + (1 - \alpha_1)\mathbf{F}_{A,B}^a(\mathbf{s}) + \alpha_2\mathbf{F}_{SP}^s(\mathbf{s}) + (1 - \alpha_2)\mathbf{F}_{SP}^a(\mathbf{s}), \quad (1)$$

$$\mathbf{M}_{SRP} = \alpha_1(1 - \mu_1)\mathbf{M}_{A,B}^d(\mathbf{s}) + \alpha_1\mu_1\mathbf{M}_{A,B}^s(\mathbf{s}) + (1 - \alpha_1)\mathbf{M}_{A,B}^a(\mathbf{s}) + \alpha_2\mathbf{M}_{SP}^s(\mathbf{s}) + (1 - \alpha_2)\mathbf{M}_{SP}^a(\mathbf{s}). \quad (2)$$

Here \mathbf{s} is the Sun vector, $\mathbf{F}()$ and $\mathbf{M}()$ in the right handed parts of

Equations (1) and (2) represent force and torque contributions from different parts of the spacecraft and different types of reflection: subscript A,B relates to the antenna and the spacecraft bus, SP — to the solar panels, superscripts d , s and a determine diffuse reflection, specular reflection and absorption of solar radiation respectively. Functions of force and torque components in the right handed parts of Equations (1) and (2) depend only on position of the Sun \mathbf{s} , therefore they are tabulated for various Sun angles to speed up the integration of equations of motion.

The complete dynamic model which is used to describe the orbital motion of the RadioAstron spacecraft is given in Table 2. Between the events of desaturation of accumulated angular momentum the spacecraft moves passively and every event of desaturation is associated with certain Delta V vector. Initial values of velocity change vectors are calculated using known attitude of the spacecraft and target Delta V value for each thrusters' firing during the desaturation provided by the attitude control system via telemetry.

3. Tracking and on-board observations

Observational data that is used in the RadioAstron orbit determination comes from different sources. The main one is standard radio tracking consisting of sequential ranging and Doppler observations conducted at C-band. This tracking is performed in two-way mode by 64-m antenna at Bear Lakes and 70-m antenna at Ussuriysk, sessions generally last several hours and are separated by 1–3 days from each other. Frequency of those sessions is much lower than one of reaction wheels' desaturations, which makes it hard to achieve required accuracy of orbit determination using only this type of data.

Other type of radio tracking observations which has a great value for navigation of the mission is closely connected to observations of the SRT. The spacecraft is not capable to store on-board all the data the space telescope receives. Thus the observational data is directly transmitted to the Earth via spacecraft's high-gain antenna during every experiment. The downlink carrier is generated using either signal the on-board hydrogen frequency standard or the uplink carrier provided by a tracking station on the Earth. The tracking stations capable to receive and record RadioAstron downlink are located in Pushchino, Russia (PRAO) and Green bank, USA (NRAO). In addition to the recording the tracking stations perform frequency measurements of received downlink signal, thereby providing accurate Doppler observations.

RadioAstron downlink always consists of 8.4 GHz and 15 GHz carriers, the latter is modulated with data signal and the former is held unmodulated. By default the tracking stations do

Perturbation	Model
Gravity	
Static	EGM-96 up to 75th degree/order
Third bodies	DE-405 Sun, Moon and planets
Earth tides	IERS-2003 conv.
General relativity	IERS-2010 conv.
Surface forces	
Solar radiation	3 parameters α_1 , μ_1 and α_2
Earth radiation	Applied (constant albedo coeff.)
Atmospheric drag	GOST R 25645.166-2004 density model
Desaturation of reaction wheels	
Direction	On-board observations from star sensors and attitude file
Delta V magnitude	Known duration for every firing and a priori thrust model

Table 2: Description of the RadioAstron dynamic model

not provide uplink signal for the spacecraft therefore almost all Doppler observations conducted by Pushchino and Green bank stations are one-way.

A comparison of a posteriori estimated radio tracking accuracy is shown in Table 3. One-way observations at Pushchino and Green bank have overall better accuracy and despite bearing an uncertainty due to on-board clocks provide great assistance to routine orbit determination.

Tracking station	Range bias, m	Doppler noise, mm/s
Bear lakes, 64-m	2.9	1.21
Ussuriysk, 70-m	13.4	4.78
Pushchino, 22-m	N/A	0.19
Green bank, 140-ft	N/A	0.04

Table 3: A posteriori estimates of radio tracking errors based on OD results from September 2016 to April 2017. Doppler observations at Bear lakes and Ussuriysk are received over 1 second integration span, at Pushchino and Green bank — normal point over 1 minute.

Described radio tracking of RadioAstron is supplemented by a tracking in optical band. Routine astrometric observations are conducted by a number of observatories including ones of the ISON, Roscosmos facilities, MASTER network and many others. More than 40 different telescopes have been observed the spacecraft so far providing angular measurements of right ascension and declination of the spacecraft.

Much more accurate but significantly less common are laser ranging observations. RadioAstron is featured with a retro-reflector array which makes it possible to obtain laser echoes from the spacecraft when it is in specific orientation. Because of rather strict attitude requirements RadioAstron laser ranging interferes with S-VLBI observations. This along with distances to the spacecraft, which are often beyond the capabilities of the majority of SLR tracking stations, obstructs frequent laser ranging. So far successful ranging has been performed by the following observatories: Grasse (France), Kavkaz (Russia), Yarragadee and Mt. Stromlo (Australia), Wettzell (Germany).

Several types of on-board observations and products proved to be helpful in the dynamics modeling and orbit determina-

tion of RadioAstron. Attitude information and characteristics of thrusters' firings are vital because they help to describe perturbations due to SRP and provide an estimate of resulting Delta V due to desaturations of reaction wheels. Additional on-board observations, which implicitly contain information about the dynamics of the spacecraft' center of mass and therefore are used in OD are observations of reaction wheels' rotation speeds.

Dynamics of the center of mass and rotation of reaction wheels, i.e. attitude dynamics, are related by the action of SRP. Given that the spacecraft attitude is the same at t_1 and t_2 and rotation with respect to an inertial frame is absent the change of the angular momentum can be represented in a body-fixed frame as

$$\sum_{i=1}^8 I_i \mathbf{a}_i (\Omega_i(t_2) - \Omega_i(t_1)) = \int_{t_1}^{t_2} \mathbf{M}(t) dt, \quad (3)$$

here I_i is the moment of inertia of i -th wheel, \mathbf{a}_i — its axis of rotation, $\Omega_i(t)$ — angular velocity of the wheel and $\mathbf{M}(t)$ is perturbing torque. Commonly SRP is the only major source of perturbing torque which is responsible for the change of angular momentum of the reaction wheels. Thereby Equation (3) allows to obtain observed value of SRP torque in a body-fixed frame if SRP variations over (t_1, t_2) span are negligible

$$\mathbf{M}_{SRP,o} = \frac{1}{t_2 - t_1} \sum_{i=1}^8 I_i \mathbf{a}_i (\Omega_i(t_2) - \Omega_i(t_1)). \quad (4)$$

Corresponding computed value of SRP torque is expressed by Equation (2). The computed value depends on introduced SRP coefficients therefore observations of reaction wheels' rotation speeds contain useful information which otherwise may only be obtained from the orbital dynamics of the RadioAstron.

4. Orbit determination technique

According to described above dynamic model of the RadioAstron spacecraft its orbital motion is determined by the fol-

lowing parameters $\mathbf{Q}_d = \{\mathbf{X}(t_0), \alpha_1, \mu_1, \alpha_2, \Delta \mathbf{v}_1, \dots, \Delta \mathbf{v}_n\}$ consisting of initial state vector of the spacecraft, SRP coefficients and vectors of velocity change due to desaturations of reaction wheels given n of such events occurred over orbit determination interval. Among kinematic parameters, affecting only computed values of observations, there are session-wise range biases and relative frequency offset of on-board hydrogen maser. The latter affects one-way Doppler observations conducted by the tracking stations, since certain downlink frequency has to be assumed on processing. Moreover the on-board frequency standard feeds the formatter that ultimately determines the local timescale against which observations of the SRT are recorded. Therefore any offset of this frequency from a nominal value would affect measurements of intervals of proper time on board of the spacecraft and thereby residual delays and delay rates obtained during a fringe search. As a result the solve-for parameters in the OD problem that are meaningful for the correlation of S-VLBI observations are dynamic parameters \mathbf{Q}_d and frequency offset (on-board clocks drift) $h = \Delta f_0 / f_0$.

Orbit determination itself has been performed using batch least squares estimator. The functional to minimize is as follows

$$\begin{aligned} \Phi = & (\Psi_o - \Psi_c)^T \mathbf{P} (\Psi_o - \Psi_c) + \\ & + \sum_{j=1}^N (\mathbf{M}_{SRP,o}^j - \mathbf{M}_{SRP}^j)^T \mathbf{P}_j^{SRP} (\mathbf{M}_{SRP,o}^j - \mathbf{M}_{SRP}^j) + \\ & + \sum_{i=1}^m (\Delta \mathbf{v}_i^0 - \Delta \mathbf{v}_i)^T \mathbf{P}_i (\Delta \mathbf{v}_i^0 - \Delta \mathbf{v}_i). \end{aligned} \quad (5)$$

The first term in Equation (5) is standard, it describes a contribution of tracking data Ψ_o with corresponding computed values Ψ_c and inverted covariance estimate of Ψ_o as weight matrix \mathbf{P} .

The second term in Equation (5) contains sum of squares of residual torques observed and computed values of which were described in the previous section (see Equations (4) and (2)). The covariance and corresponding weight matrices \mathbf{P}_{SRP}^j can be estimated using Equation (4) and error estimates of rotation speeds of reaction wheels and alignment of their axes. Yet in practice the weight has to be adjusted to the accuracy level of about $2 \cdot 10^{-6}$ N·m·s, since the model of perturbing torque described above is rather simple and hinders matching the actual accuracy of the observations. Fig. 1 shows how modeled torque in general agrees with observational data. As seen from the figure relative agreement of X and Z components is significantly lower than one of Y component, but the latter holds the major part of the torque and about an order of magnitude greater than the others.

The last term of Equation (5) takes into account a priori information about velocity changes due to reaction wheels' desaturations. For each event of desaturation the value of net $\Delta \mathbf{v}_i^0$ is calculated using information about every occurred thrusters' firing namely a duration, fuel tank pressure and a priori thrust model [Zakhvatkin et al. \(2014\)](#). Each weight matrix \mathbf{P}_i in (5) is an inverse of covariance matrices of the following form

$$\mathbf{K} = \sigma_d^2 (\mathbf{E} - \mathbf{e} \cdot \mathbf{e}^T) + \sigma_m^2 \mathbf{e} \cdot \mathbf{e}^T.$$

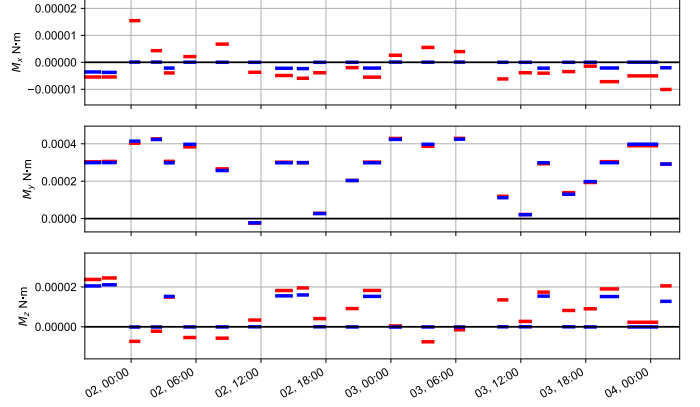


Figure 1: Observed (red) and computed (blue) SRP torques during periods of constant attitude over 48 hours interval

Here \mathbf{e} is the unit vector of $\Delta \mathbf{v}$ which has the same direction as X -axis of the spacecraft, \mathbf{E} is identity matrix of size 3, σ_m is the error of the estimate of Δv magnitude, and σ_d is the error of magnitude error σ_m in the plane orthogonal to \mathbf{e} . The used value of component σ_d corresponds to 0.25 degree offset from the nominal direction or $4.36 \cdot 10^{-3}$ of Δv .

In reality the functional is not limited to the one in (5). It accounts also for a priori information on range biases and on-board frequency offset. The problem of finding optimal estimate of orbital parameters is solved iteratively with standard methods. It should be noted that the solution does not require an integration of additional variational equations for dynamical parameters $\Delta \mathbf{v}_i$, all the necessary partial derivatives are calculated by means of only transition matrix $\partial \mathbf{X} / \partial \mathbf{X}_0$.

5. Orbit determination results

The orbit determination algorithm outlined in this paper has been implemented and used by Keldysh Institute of Applied Mathematics (KIAM) to supply the RadioAstron users with a posteriori orbit data required for the correlation of the signals observed by the RadioAstron spacecraft and ground based observatories. All the experiments with the RadioAstron since 2014 primarily used that orbit data for correlation. Significant part of experiments conducted before 2014 has been re-correlated using new orbit data.

The main users of the obtained orbital solutions are correlators involved in a processing of the data received by the spacecraft and ground based VLBI stations during experiments with RadioAstron. The correlator having the largest statistics of processed experiments belongs to Astro Space Center of Lebedev Physical Institute (ASC) [Likhachev et al. \(2017\)](#) the leading organization of the RadioAstron project. Our goal is to evaluate orbit determination accuracy using the correlator's output and compare it with another estimates.

As it was mentioned above a statistically significant correlation found between signals recorded at the RadioAstron spacecraft and at a ground based VLBI station yields residual values of delay and delay rate. In this paper we will focus on the delay

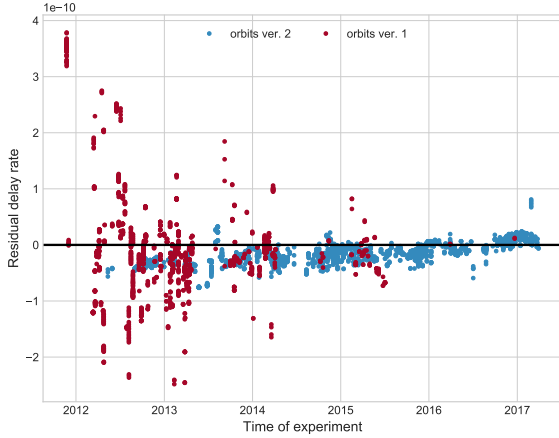


Figure 2: Residual delay rates obtained by ASC correlator using different orbit data: blue dots correspond to orbits obtained with the new algorithm (ver. 2), red dots — orbits with generic algorithm (ver. 1)

rate data only for the following reasons. The indirect synchronization (by means of a tracking station) of the RadioAstron time tagging with UTC, non zero probability of inconsistent UTC synchronization parameters of VLBI stations and significant orbit unrelated sources of residual delay rate make it impossible with high degree of certainty to separate geometrical residual delay due to orbital errors from the delay due to clocks of the involved ground and space stations. On the other hand the causes of the residual delay rate are much more predictable. Synchronization via a tracking station does not affect delay rate since additional delay caused by it remains constant during the processed scan. Clock drift for a ground based VLBI station is generally at least 2 orders of magnitude smaller than observed residual delay rate, and the spacecraft clock drift can be estimated independently during orbit determination process.

Fig. 2 shows residual delay rates obtained by ASC correlator on experiments with RadioAstron which have been carried up to early 2017. Each dot corresponds to significant in terms of SNR correlation detection between RadioAstron and one of the largest ground based antennas, including Arecibo, Effelsberg, GBT-VLBA, Westerbork, Yebes and others, obtained using different sources of the orbital data. All the experiments related to Fig. 2 were conducted in the so called “one-way mode” in which two following important conditions are met: all science systems on the spacecraft obtain reference signal from the on-board H-maser, the reference signal for the downlink carrier, which is used to transfer the science data from the spacecraft to a tracking station, is also generated using reference H-maser signal.

In the data represented in Fig. 2 the RadioAstron spacecraft is always considered as the first antenna while a ground based telescope as the second one. Residual delay rates obtained using orbits (version 1) produced with the generic algorithm which was primarily used before 2014 are depicted with red color, the rates obtained on orbits (version 2) produced by the algorithm described in this paper (which further will be referred

to as version 2) are colored with blue.

Variations of the residual delay rates achieved with version 2 algorithm are substantially lower than ones obtained with generic algorithm. Corresponding RMS values of delay rates are 2.463×10^{-11} and 1.097×10^{-10} respectively. Residual delay rates obtained with version 2 orbits however has some significant bias their average value is 1.663×10^{-11} (see Fig. 3). This indicates a systematic affect, which is hardly related directly to the orbit errors, since the residual values were obtained with large number of independent orbit solutions in experiments with different combination of baselines and observed radio sources.

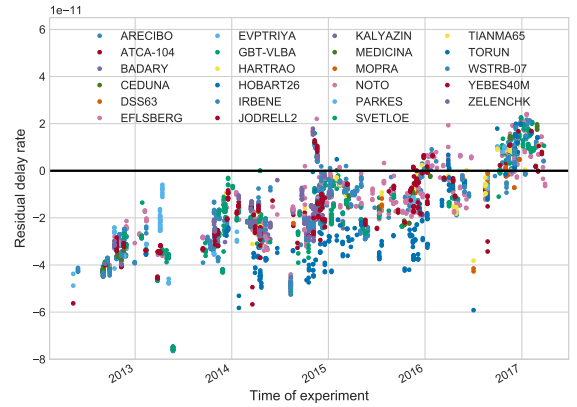


Figure 3: Residual delay rates on orbits obtained with version 2 OD algorithm received from the ASC correlator and grouped by the second station operating with the spacecraft

In order to separate orbit related errors and systematic effects due to stations clocks from the residual delay rates consider the VLBI delay model [Petit and Luzum \(2010\)](#) which is implemented in the ASC correlator. According to it a correction to computed geocentric delay, which takes account for error in a priori geocentric baseline and non-zero clock drifts of receiving stations, would be as follows

$$\delta((t_2 - t_s)_p - (t_1 - t_s)_p) = -\frac{\frac{\mathbf{K} \cdot \delta \mathbf{b}}{c}}{1 + \frac{\mathbf{K} \cdot (\mathbf{V}_\oplus + \mathbf{v}_2)}{c}} + \frac{\mathbf{V}_\oplus \cdot \delta \mathbf{b}}{c^2} - \int_{t_s}^{t_1} h_1(t) dt + \int_{t_s}^{t_2} h_2(t) dt. \quad (6)$$

Here t_i is geocentric time of wavefront arrival to i -th station, t_s is geocentric synchronization time, \mathbf{K} is the unit vector towards a radio source in the barycentric frame, \mathbf{V}_\oplus is the barycentric velocity of the geocenter, \mathbf{v}_2 is geocentric velocity of the station #2, $\delta \mathbf{b} = \delta \mathbf{r}_2(t_1) - \delta \mathbf{r}_1(t_1)$ is a variation in the geocentric baseline vector, h_1 and h_2 are corresponding clock drifts of station #1 and #2 respectively. Introduced clock drifts account only for instrumental effects, i.e. describe how 1 second interval of proper time measured by station clocks differs from TAI second.

The correction to computed delay rate is the time derivative of Equation (6). Given that the position and velocity of participating ground based station #2 are known much better than the state of the spacecraft and the drift h_2 of its clocks is of order of 10^{-13} or less the corresponding terms can be omitted during differentiation. Therefore the correction to delay rate for convenience multiplied by the speed of light is as follows

$$c \cdot \frac{d}{dt} \delta((t_2 - t_s)_p - (t_1 - t_s)_p) = \mathbf{k} \cdot \delta \mathbf{v}_1 - c \cdot h_1(t_1), \quad (7)$$

here \mathbf{k} is the unit vector of aberrated direction to a radio source and $\delta \mathbf{v}_1$ is the error of a priori spacecraft velocity evaluated at t_1 .

Assuming absence of other systematic effects each data point showed in Fig. 2 corresponds to an evaluation of Equation (7) at a certain time on a certain a priori orbit (since residual value includes calculated delay rate with negative sign) plus an error of residual delay rate determination via correlation itself. That is after corrected for the drift of the on-board clocks the data on Fig. 2 will represent according to Equation (7) spacecraft velocity error projected on the direction of observed source.

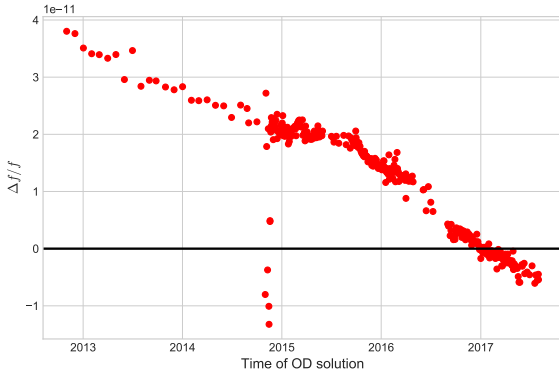


Figure 4: Estimated values of the on-board hydrogen maser relative frequency offset

Delay model implemented in the ASC correlator assumes that the spacecraft clocks are ideal and $h_1(t) = 0$. Therefore any instrumental effect affecting the clock drift if present would manifest itself in the resulting delay rates provided by the correlator.

It was emphasized above that all the experiments, correlation in which is analyzed, have been conducted in the mode where both spacecraft clocks and downlink carrier transmitted from the RadioAstron spacecraft to a tracking station uses H-maser signal as reference. A tracking station measures frequency of the received downlink, thereby providing one-way Doppler observations. These observations are used by the OD team in addition to the data provided by standard tracking techniques.

In order to properly fit one-way Doppler during OD we had to take into account frequency biases of both H-masers participating in an observation: spacecraft H-maser and H-maser of a tracking station. We estimated the relative frequency bias of the spacecraft downlink, and thus H-maser, along with other orbit

parameters during OD. For a tracking station we used a priori value of frequency bias derived from long series of measured difference between station local time and GNSS time.

The values of the spacecraft H-maser relative frequency bias obtained during OD are shown in Fig. 4. On more than 4 year time span the offset demonstrates close to linear change over time. In late October 2014 an accident occurred during which the on-board H-maser experienced power surge every time the C-band transponder was turned on. Before the accident the frequency offset has been assumed constant on the whole orbit determination interval. After the accident the frequency bias has been separately estimated for every interval between C-band transponder switching, which usually coincided with radio tracking from Bear Lakes or Ussuriysk stations. It explains the change of the data points density on Fig. 4 before and after October 2014.

Using the connection between downlink carrier and spacecraft clocks we can assert that $\Delta f/f = h_1$ and use the determined value of relative frequency bias to correct residual delay rates according to Equation (7). The residual delay rates before the correction are shown on Fig. 3. The residuals after application of the estimated clock correction are shown on Fig. 5. After the correction the RMS of residual delay rates reduced to 1.239×10^{-11} and its mean value reduced from 1.663×10^{-11} to 3.735×10^{-12} .

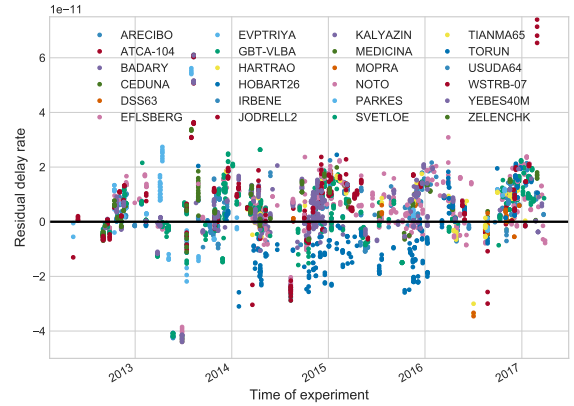


Figure 5: Residual delay rates with the correction for instrumental drift of the spacecraft clocks

The residual delay rates obtained after application of the correction on the spacecraft clock drift according to Equation (7) should represent a projection of spacecraft velocity error to the direction of observed radio source. However the resulted values are still have significant systematic expressed in bias of about 1.12 mm/sec and variations with period about 1 year. How the distribution on residuals is biased can be seen on the left part of Fig. 6.

The periodic variations seen at Fig. 5 are contained by the original data and have not been introduced with the clocks correction $h_1(t)$. In attempt to find cause of the periodicity in the

delay rates corrected for the spacecraft clock drift we tried several hypotheses. Among them more probable seemed those ones that relate the effect to the clocks rather than to the spacecraft velocity errors, because in every experiment the velocity error $\delta\mathbf{v}_1$ is evaluate along pseudo-random direction \mathbf{k} in (7). The latter requires a complex relation between spacecraft velocity error and observed radio source to produce the periodic dependence in corresponding dot product of two vectors.

We found that the initial data may be improved with the following correction to the residual delay rates

$$\delta\tau = \frac{\mu_{\odot}}{c^2} \left(\frac{1}{R} - \frac{1}{R_{\oplus}} \right), \quad (8)$$

where μ_{\odot} is the gravitational parameter of the Sun, R is the heliocentric distance to the RadioAstron spacecraft during an experiment and R_{\oplus} is the heliocentric distance to the Earth during an experiment. The expression (8) contains difference in time dilation due to gravity of the Sun between observers at the geocenter and at the location of the spacecraft.

Application of the correction (8) to the residual delay rates can also be treated as subtraction of the same expression from computed value of delay rate. That is if the time dilation due to the Sun's gravity between the spacecraft and a VLBI station on Earth has been taken into account by the delay model the correction (8) would cancel this.

The residual delay rate after application of the correction (8) are shown at Fig. 7. In addition to overall reduction of delay rate variations this correction shows that a part of data points corresponding to correlation between the RadioAstron spacecraft and Torun telescope have bias about 1.9×10^{-11} , which is probably related to the VLBI station clocks.

After excluding the Torun data points (8.2% of all data) the mean value of residual delay rates of the rest data set on Fig. 7 has reduced to 4.387×10^{-13} and its RMS to 9.573×10^{-12} . The residual rates also became less biased as could be seen comparing histograms on the left and right parts of Fig. 6.

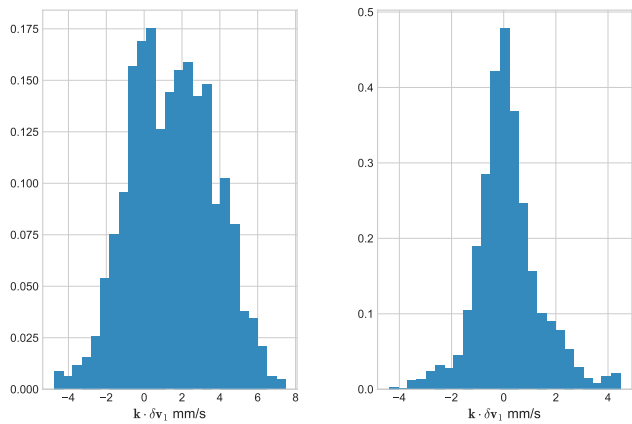


Figure 6: Histogram of the residual delay rates (experiments with Torun are excluded) after application of the correction for the spacecraft clock drift (left) and additional correction for the time dilation due to the Sun's gravity (right)

To investigate further statistical properties of the residual delay rates 7 we excluded the data corresponding to experiments conducted in summer, i.e. between 1st of June and 1st of September. These experiments make up 10.4% of the data, but, as can be seen at Fig. 7, give much higher residual delay rates — with RMS equal to 2.307×10^{-11} , which is more than 5 times higher than one for the rest of the data. Lower orbit determination accuracy is definitely one of the main reasons for summer experiments having larger residual delay rates. The number of experiments with the RadioAstron drops significantly during summer because of many factors the major of which are due to constraints on the spacecraft attitude with respect to the Sun and thus on visibility of radio sources of interest. The lack of experiments reduces the amount of Doppler data from tracking stations available to the OD team which in turn affects the orbit accuracy.

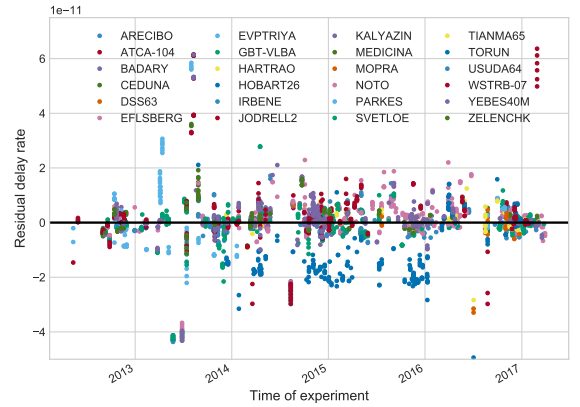


Figure 7: Residual delay rates after application of corrections for the spacecraft clock drift and time dilation due to the Sun's gravity

The residual delay rates data with excluded summer experiments and several outliers (1.15% of the initial data points larger than 5σ threshold) make up 88.4% of the initial data set. Residual delay rates within this set have mean value equal to 4.428×10^{-13} and RMS equal to 4.255×10^{-12} . This corresponds to the standard deviation of the spacecraft velocity error projection $\mathbf{k} \cdot \delta\mathbf{v}_1$ equal to 1.275 mm/s.

We have obtained an estimate of the spacecraft velocity error projection onto the observed source direction $\mathbf{k} \cdot \delta\mathbf{v}_1$ under the assumptions that the clock drift of participating ground based VLBI station is small, the spacecraft clock drift is equal to the estimated value of relative frequency bias of the spacecraft H-maser and correction (8) is required to remove probable inconsistencies between orbit and delay models. In order to obtain more information about spacecraft velocity error $\delta\mathbf{v}_1$ rather than its projection $\mathbf{k} \cdot \delta\mathbf{v}_1$ we represented the residual delay rates as a function of the angle α between direction \mathbf{k} and direction to a tracking station during an experiment.

Since every experiment within this data set has been supported with simultaneous Doppler observations from a tracking station we can assume that the largest velocity errors in recon-

structed orbits are expected in the directions orthogonal to the direction to a tracking station, and contrary, errors should be the smallest for directions, which are close to the direction to a tracking station. In contrast Fig. 8 shows that dependence of the velocity error $\delta \mathbf{v}_1$ (evaluated along direction \mathbf{k}) on the angle α is rather weak.

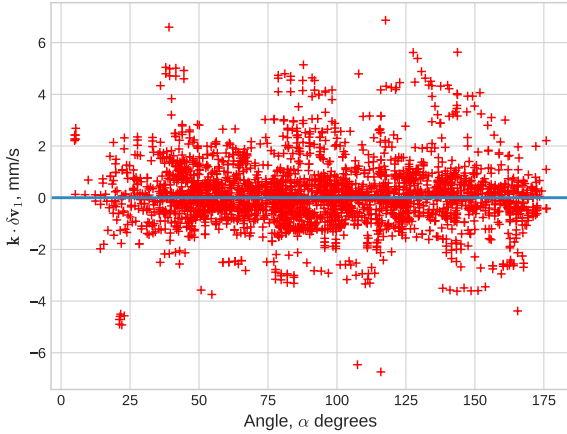


Figure 8: Dependence of residual delay rates on the angle between the direction to observed source and direction from the spacecraft to a tracking station

From that we can estimate the velocity error along the “worst” directions. To obtain the value we picked the experiments where $75^\circ \leq \alpha \leq 105^\circ$. For those experiments the RMS of $\mathbf{k} \cdot \delta \mathbf{v}_1$ is 1.359 mm/s. Assuming the spacecraft velocity is determined better along other direction the error ellipsoid of $\delta \mathbf{v}_1$ vector is limited by covariance matrix $\text{diag}(1.84 \text{ mm}^2/\text{s}^2, 1.84 \text{ mm}^2/\text{s}^2, 1.84 \text{ mm}^2/\text{s}^2)$.

To obtain independent estimate of the error we performed a comparison of 42 independent adjacent orbit solutions from 2014 to 2017 for discontinuity in velocity. Given that the one solution was obtained on the interval (t_1, t_2) and the other one on the interval (t_2, t_3) the comparison of the determined orbital state vector was performed at the time t_2 . The RMS (3D) of velocity difference at 41 examined points turned to be 3.20 mm/s. However the considered difference is also the difference between orbital errors of two independent orbital solutions, therefore its variance is described by the sum of variances of both solutions. Thus we consider that the estimated 3D RMS of the velocity error of a single orbital solution is about 2.26 mm/s. Two estimates of the total velocity error of reconstructed orbits provide results of the same order.

6. Discussion

Obtained estimate of velocity errors seem reasonable and self-consistent. However in order to extract it from the residual delay rate data we performed two major corrections to the data. The first one corresponds to taking into account instrumental drift of the spacecraft clocks. It is justified because the downlink frequency bias (related to the spacecraft H-maser frequency bias) becomes evident when one-way Doppler data is

processes along with two-way range and Doppler observations of the spacecraft and ASC delay model assumes the clocks are ideal. This correction also introduces additional errors to the data since downlink frequency bias is determined not precisely during OD.

The second correction described by equation (8) greatly improves the residual rates data. The reconstructed orbits provided to the correlator are set in geocentric frame and corresponding timescale TT, therefore there is no need to take into account the gravitational field of the Sun when calculating intervals of proper time on board of the spacecraft and at the Earth within delay model. That is a difference between time and coordinate systems used to describe reconstructed orbits and ones expected by the implemented delay model could be a plausible explanation for the need of the correction (8). Resolving this issue will probably allow to expand this study on the delay data.

7. Conclusion

In this paper we outlined the method of the RadioAstron orbit determination which is used for provision of the primary orbital information for the RadioAstron data users. The method incorporates the developed SRP model which allows to utilize on-board observations of accumulated angular momentum of reaction wheels improving thereby the knowledge of the dynamics of the spacecraft’s center of mass. The accuracy performance of the OD method has been tested using residual delay rates data provided by the ASC correlator as a result of processing the observational data from experiments with RadioAstron. It showed that the described method provides about 11 times more accurate solution in terms delay rate than generic method that utilizes simplified SRP model. The residual delay rates obtained in non-summer experiments, which make up 88.4% of all data, provide the estimate for standard deviation of the spacecraft velocity error. It is less or equal to 1.359 mm/s for every component of the velocity. Obtained results are in agreement with independent a posteriori estimate of the orbit error via discontinuity analysis, which shows 3D RMS of the velocity error equals to 2.26 mm/s.

8. Acknowledgements

The work of MVZ is supported by the RSF grant 17-12-01488 (evaluation of RadioAstron orbit determination accuracy for RadioAstron gravitational redshift experiment). The RadioAstron project is led by the Astro Space Center of the Lebedev Physical Institute of the Russian Academy of Sciences and the Lavochkin Scientific and Production Association under a contract with the Russian Federal Space Agency, in collaboration with partner organizations in Russia and other countries including Keldysh Institute of Applied Mathematics of the Russian Academy of Sciences.

References

- N. S. Kardashev, et al., “radioastron”-a telescope with a size of 300 000 km: Main parameters and first observational results, *Astronomy Reports* 57 (2013) 153–194. doi:[10.1134/S1063772913030025](https://doi.org/10.1134/S1063772913030025).
- D. Litvinov, V. Rudenko, A. Alakoz, U. Bach, N. Bartel, A. Belonenko, K. Belousov, M. Bietenholz, A. Biriukov, R. Carman, G. Cim, C. Courde, D. Dirx, D. Duev, A. Filetkin, G. Granato, L. Gurvits, A. Gusev, R. Haas, G. Herold, A. Kahlon, B. Kanevsky, V. Kauts, G. Kopelyansky, A. Kovalenko, G. Kronschnabl, V. Kulagin, A. Kutkin, M. Lindqvist, J. Lovell, H. Marley, J. McCallum, G. M. Calvs, C. Moore, K. Moore, A. Neidhardt, C. Pitz, S. Pogrebenko, A. Pollard, N. Porayko, J. Quick, A. Smirnov, K. Sokolovsky, V. Stepanyants, J.-M. Torre, P. de Vicente, J. Yang, M. Zakhvatkin, Probing the gravitational redshift with an earth-orbiting satellite, *Physics Letters A* 382 (2018) 2192 – 2198. doi:<https://doi.org/10.1016/j.physleta.2017.09.014>, special Issue in memory of Professor V.B. Braginsky.
- M. V. Zakhvatkin, Y. N. Ponomarev, V. A. Stepanyants, A. G. Tuchin, G. S. Zaslavsky, Navigation support for the radioastron mission, *Cosmic Research* 52 (2014) 342–352. doi:[10.1134/S0010952514050128](https://doi.org/10.1134/S0010952514050128).
- S. F. Likhachev, V. I. Kostenko, I. A. Girin, A. S. Andrianov, A. G. Rudnitskiy, V. E. Zharov, Software Correlator for Radioastron Mission, *Journal of Astronomical Instrumentation* 6 (2017) 1750004–131. doi:[10.1142/S2251171717500040](https://doi.org/10.1142/S2251171717500040). [arXiv:1706.06320](https://arxiv.org/abs/1706.06320).
- G. Petit, B. Luzum, IERS Conventions (2010), Technical Report, Verlag des Bundesamts fr Kartographie und Geodsie, 2010. IERS Technical Note ; 36.